THE JOURNAL OF BIOLOGICAL CHEMISTRY VOL. 288, NO. 25, pp. 18300–18310, June 21, 2013

The Yeast ATP-binding Cassette (ABC) Transporter Ycf1p Enhances the Recruitment of the Soluble SNARE Vam7p to Vacuoles for Efficient Membrane Fusion*

Received for publication, November 29, 2012, and in revised form, May 6, 2013 Published, JBC Papers in Press, May 8, 2013, DOI 10.1074/jbc.M112.441089

Terry L. Sasser, Gus Lawrence[1], Surya Karunakaran, Christopher Brown, and Rutilio A. Fratti[2]

From the Department of Biochemistry, University of Illinois at Urbana-Champaign, Urbana, Illinois 61801

Background: Ycf1p is a ABCC transporter that is localized to the vacuole and that was initially characterized as a cadmium transporter.
Results: Deletion of *YCF1* inhibits vacuole fusion in part by excluding the soluble SNARE Vam7p.
Conclusion: The vacuole fusion machinery requires Ycf1p function for efficient fusion.
Significance: This is the first report that an ABCC protein affects fusion through the recruitment of a SNARE.

The *Saccharomyces cerevisiae* vacuole contains five ATP-binding cassette class C (ABCC) transporters, including Ycf1p, a family member that was originally characterized as a Cd^{2+} transporter. Ycf1p has also been found to physically interact with a wide array of proteins, including factors that regulate vacuole homeostasis. In this study, we examined the role of Ycf1p and other ABCC transporters in the regulation of vacuole homotypic fusion. We found that deletion of *YCF1* attenuated *in vitro* vacuole fusion by up to 40% relative to wild-type vacuoles. Plasmid-expressed wild-type Ycf1p rescued the deletion phenotype; however, Ycf1p containing a mutation of the conserved Lys-669 to Met in the Walker A box of the first nucleotide-binding domain ($Ycf1p^{K669M}$) was unable to complement the fusion defect of *ycf1*Δ vacuoles. This indicates that the ATPase activity of Ycf1p is required for its function in regulating fusion. In addition, we found that deleting *YCF1* caused a striking decrease in vacuolar levels of the soluble SNARE Vam7p, whereas total cellular levels were not altered. The attenuated fusion of *ycf1*Δ vacuoles was rescued by the addition of recombinant Vam7p to *in vitro* experiments. Thus, Ycf1p contributes in the recruitment of Vam7p to the vacuole for efficient membrane fusion.

Eukaryotic homeostasis requires the packaging, trafficking, and delivery of membrane-bound cargo between organelles. The final stage of these pathways occurs through the fusion of two membranes, which is catalyzed by a core set of machinery that is conserved throughout eukaryotes (1). To study the regulation of membrane fusion, we used vacuoles (lysosomes) from *Saccharomyces cerevisiae*. Vacuole fusion requires the Rab GTPase Ypt7p and its effector complex HOPS (homotypic fusion and vacuole protein sorting), which tether membranes together. The final stage of fusion is catalyzed by SNARE proteins, which interact across the docking junction to form parallel four-helix bundles that deform and destabilize membranes to trigger fusion. The function of these proteins is regulated by a group of lipids that include ergosterol, diacylglycerol, phosphatidic acid, and phosphoinositides (2). These lipids and proteins interdependently form specialized membrane raft microdomains called vertices to create the site of fusion (3–5).

Studies that use reconstituted proteoliposomes as a model for fusion have identified the minimum fusion machinery; however, in biological systems, the fusion machinery has to be highly regulated through various pathways. Vacuole homotypic fusion is regulated by various factors, including the casein kinase Yck3p (6); the lipid modifiers Pah1p (7), Plc1p (8), and Vps34p (9); and the Na^+/H^+ exchanger Nhx1p (10). We recently found that the ATP-binding cassette class C (ABCC)[3] transporter Ybt1p negatively regulates fusion through the control of Ca^{2+} transport across the vacuole membrane (11). Ybt1p also translocates phosphatidylcholine across the vacuole bilayer for degradation and choline recycling (12).

Ybt1p is one of the five confirmed ABCC transporters that reside on the vacuole membrane and was initially discovered as an ATP-dependent bile acid transporter (13). The other yeast vacuole ABCC proteins include the yeast cadmium factor Ycf1p (14, 15), the bile acid transporter Bpt1p (16), and the less well characterized Vmr1p and Nft1p (17). Aside from the transport of cadmium, Ycf1p has been reported to physically interact with various vacuolar proteins that are linked to membrane trafficking and fusion, including the phosphatidylinositol 3-phosphate (PI3P) 5-kinase Fab1p (18). In this study, we examined the role of Ycf1p and other ABCC transporters in vacuole fusion. We found that deletion of *YCF1* strongly attenuated fusion by reducing the vacuole association of the soluble SNARE Vam7p.

* This work was supported, in whole or in part, by National Institutes of Health Grant GM101132 (to R. A. F.). This work was also supported by a grant from the University of Illinois Research Board (to R. A. F.).
[1] Supported by a National Science Foundation-Cellular and Molecular Mechanics and BioNanotechnology Integrative Graduate Education Research Training fellowship.
[2] To whom correspondence should be addressed: Dept. of Biochemistry, University of Illinois at Urbana-Champaign, 419 Roger Adams Laboratory, B-4, 600 S. Mathews Ave., Urbana, IL 61801. Tel.: 217-244-5513; Fax: 217-244-5858; E-mail: rfratti@illinois.edu.

[3] The abbreviations used are: ABCC, ATP-binding cassette class C; PI3P, phosphatidylinositol 3-phosphate; CBP, calmodulin-binding peptide; Rh-PE, rhodamine-conjugated phosphatidylethanolamine; TAP, tandem affinity purification; CFTR, cystic fibrosis transmembrane conductance regulator.

TABLE 1
Yeast strains used in this study

Strain	Genotype	Source
BJ3505	*MATa pep4::HIS3 prb1-Δ1.6R his3 lys2-208 trp1Δ101 ura3-52 gal2 can1*	Ref. 56
DKY6281	*MATα pho8::TRP1* leu2-*3 leu2-112 ura3-52 his3-Δ200 trp1-Δ901 lys2-801*	Ref. 57
BJ3505 CBP-Vam3p *nyv1Δ*	BJ3505, *CBP-VAM3::Kan*^{r} *nyv1Δ::nat*^{r}	Ref. 26
BY4741	MAT**a** *his3Δ1 leu2Δ0 ura3Δ0 met15Δ0*	Open Biosystems
Ycf1p-TAP	MAT**a** *his3Δ1 leu2Δ0 ura3Δ0 met15Δ0 YCF1*::TAP-*URA3*	Open Biosystems
RFY32	BJ3505, *ycf1Δ::kanMX6*	This study
RFY33	DKY6281, *ycf1Δ::kanMX6*	This study
RFY34	BJ3505, *bpt1Δ::kanMX6*	This study
RFY35	DKY6281, *bpt1Δ::kanMX6*	This study
RFY36	BJ3505, *ycf1Δ::URA3 bpt1Δ::TRP1*	This study
RFY37	DKY6281, *ycf1Δ::URA3 bpt1Δ::HIS3*	This study
RFY38	RFY36, *ybt1Δ::kanMX6*	This study
RFY39	RFY37, *ybt1Δ::kanMX6*	This study
RFY40	BJ3505, *nft1Δ::hphMX4*	This study
RFY41	DKY6281, *nft1Δ::hphMX4*	This study
RFY42	BJ3505, *vmr11Δ::hphMX46*	This study
RFY43	DKY6281, *vmr11Δ::hphMX4*	This study
RFY44	BJ3505, *yol075c1Δ::hphMX4*	This study
RFY45	DKY6281, *yol075c1Δ::hphMX4*	This study
RFY46	DKY6281, *YCF1*::GFP	This study
RFY47	DKY6281, *BPT1*::GFP	This study
RFY48	DKY6281, *NFT1*::GFP	This study
RFY49	DKY6281, *VMR1*::GFP	This study
RFY50	DKY6281, *YOL075c*::GFP	This study
RFY51	RFY32, p*YCF1*	This study
RFY52	RFY33, p*YCF1*	This study
RFY53	RFY32, p*YCF1*^{K669M}	This study
RFY54	RFY33, p*YCF1*^{K669M}	This study
RFY55	BJ3505, CBP-*VAM3 nyv1Δ ycf1Δ::hghMX4*	This study
RFY56	RFY32, pGFP-FYVE	This study
RFY57	RFY33, pGFP-FYVE	This study
RFY58	BJ3505, pGFP-FYVE	This study
RFY59	DKY6281, pGFP-FYVE	This study

EXPERIMENTAL PROCEDURES

Reagents—Reagents were dissolved in PS buffer (20 mM PIPES-KOH (pH 6.8) and 200 mM sorbitol). The recombinant proteins GST-FYVE (19) and GST-Vam7p (20, 21) were prepared as described and stored in PS buffer with 125 mM KCl. The FYVE domain was labeled with Cy5 *N*-hydroxysuccinimide ester (GE Healthcare) according to the manufacturer's protocol. The MARCKS (myristoylated alanine-rich C kinase substrate) effector domain peptide was prepared as described previously (3).

Strains—BJ3505 and DKY6281 were used for fusion assays (Table 1) (22). *YCF1* was deleted from BJ3505 and DKY6281 by homologous recombination with the *kanMX6* cassette using PCR products amplified from pFA6a-*kanMX6* (23) with homology flanking the *YCF1* coding sequence. The PCR product was transformed into BJ3505 and DKY6281 by standard lithium acetate methods and plated on YPD (yeast extract/peptone/dextrose) medium containing G418 (250 μg/liter) to generate BJ3505 *ycf1Δ::kanMX6* (RFY32) and DKY6281 *ycf1Δ::kanMX6* (RFY33). Similarly, *BPT1* was deleted from BJ3505 and DKY6281 to generate BJ3505 *bpt1Δ::kanMX6* (RFY34) and DKY6281 *bpt1Δ::kanMX6* (RFY35). To generate *ycf1Δ*/*bpt1Δ* strains, *YCF1* was deleted from BJ3505 and DKY6281 with the *URA3* cassette. *BPT1* was then deleted with *TRP1* to generate RFY36 or with *HIS3* to generate RFY37. *YBT1* was deleted from RFY36 and RFY37 with *kanMX6* to generate RFY38–39. Deletions of *NFT1*, *VMR1*, and *YOL075c* were generated using PCR products amplified from pAG32 to generate *nft1Δ::hphMX4* (RFY40–41), *vmr1Δ::hphMX4* (RFY42–43), and *yol075cΔ::hphMX4* (RFY44–45) (24). For vacuole localization studies, *YCF1*, *BPT1*, *NFT1*, *VMR1*, and *YOL075c* were fused in frame to GFP by homologous recombination. DKY6281 was transformed with a PCR product amplified from pFA6a-GFP-*kanMX6* (23) with homology flanking the stop codon of the gene to generate RFY46 (DKY6281 *YCF1*::GFP), RFY47 (DKY6281 *BPT1*::GFP), RFY48 (DKY6281 *NFT1*::GFP), RFY49 (DKY6281 *VMR1*::GFP), and RFY50 (DKY6281 *YOL075c*::GFP). For complementation studies, WT *YCF1* and *YCF1*^{K669M} were subcloned from pRS424 vectors (a gift from Dr. W. Scott Moye-Rowley, University of Iowa) into pRS416 using KpnI and ScaI. RFY32 and RFY33 were transformed with p*YCF1* or p*YCF1*^{K669M} to generate RFY51–54. *YCF1* was deleted from BJ3505 CBP-Vam3p *nyv1Δ* with the *hghMX4* cassette using PCR product amplified from pAG32 with homology flanking the *YBT1* coding sequence. The PCR product was transformed into BJ3505 CBP-Vam3p *nyv1Δ* by standard lithium acetate methods and plated on YPD medium containing hygromycin (250 μg/ml) to generate BJ3505 CBP-Vam3p *nyv1Δ ybt1::hghMX4* (RFY55). WT and *ycf1Δ* strains were transformed with the pRS424-GFP-FYVE plasmid (Addgene) and grown on selective medium lacking uracil to generate RFY56–59.

Vacuole Isolation and in Vitro Vacuole Fusion—Vacuoles were isolated by floatation as described (22). Standard *in vitro* fusion reactions (30 μl) contained 3 μg each of vacuoles from the BJ3505 and DKY6281 backgrounds, fusion reaction buffer (20 mM PIPES-KOH (pH 6.8), 200 mM sorbitol, 125 mM KCl, and 5 mM $MgCl_2$), and ATP-regenerating system (1 mM ATP, 0.1 mg/ml creatine kinase, and 29 mM creatine phosphate), 10 μM CoA, and 283 nM inhibitor of protease B (IB_2). Reactions were incubated at 27 °C, and Pho8p activity was assayed in 250 mM Tris-Cl (pH 8.5), 0.4% Triton X-100, 10 mM $MgCl_2$, and 1

mM *p*-nitrophenyl phosphate. Fusion units were measured by determining the *p*-nitrophenolate produced per min/μg of *pep4*Δ vacuole, and absorbance was detected at 400 nm.

Lipid Mixing—Lipid mixing assays were conducted using rhodamine B-conjugated phosphatidylethanolamine (Rh-PE; Invitrogen) as described (7). Briefly, BJ3505 background vacuoles (300 μg) were incubated in 400 μl of PS buffer containing 150 μM Rh-PE (10 min, 4 °C, nutating). Samples were mixed with 15% (w/v) Ficoll in PS buffer and transferred to an ultracentrifuge tube. Samples were overlaid with 1.0 ml each of 8, 4, and 0% Ficoll. Labeled vacuoles were re-isolated by centrifugation (105,200 × *g*, 25 min, 4 °C) and harvested from the 0–4% Ficoll interface. Lipid mixing assays (90 μl) contained 2 μg of Rh-PE-labeled vacuoles and 16 μg of unlabeled vacuoles in fusion reaction buffer and were transferred to a black half-volume 96-well flat-bottom microtiter plate with a nonbinding surface (Corning). Rhodamine fluorescence was measured using a POLARstar Omega fluorescence plate reader (BMG Labtech) at 27 °C. Measurements were taken every minute for 75 min, yielding fluorescence values at the onset (F_0) and during the reaction (F_t). The final 10 measurements of reactions after the addition of 0.33% (v/v) Triton X-100 were averaged and used as a value for the fluorescence after infinite dilution (F_{TX100}). The relative total fluorescence change ($\Delta F_t/F_{TX100} = (F_t - F_0)/F_{TX100}$) was calculated.

Microscopy—Vacuole morphology was monitored by incubating yeast cells with YPD broth containing FM® 4-64 (Invitrogen) as described previously (11). Images were acquired using a Zeiss Axio Observer Z1 inverted microscope equipped with an X-Cite 120XL light source, a Plan Apochromat 63× oil objective (numeric aperture of 1.4), and an AxioCam CCD camera. Vertex assembly reactions were performed as described (3). Docking reactions (30 μl) contained 6 μg of vacuoles. PI3P was labeled with 0.2 μM Cy5-FYVE and used as a marker for vertex microdomains (7). Reactions were incubated at 27 °C for 30 min, placed on ice, and stained with 3 μM MDY-64. Reactions were next mixed with low melting agarose, vortexed to disrupt spurious clustering, and mounted on slides for observation by fluorescence microscopy. Statistical analysis of Cy5-FYVE enrichment at vertices was done using JMP 5 (SAS Institute Inc.). Ratio data were log-transformed before analysis to yield near-normal distributions with comparable variances. Ratio means and 95% confidence intervals were analyzed using one-way analysis of variance. Significant differences were determined using *t* test and corrected for multiple comparisons using the Dunn-Sidak method (25). p values <0.05 were considered significant.

Quantitative PI3P ELISA—Total levels of PI3P were determined using a quantitative ELISA (Echelon, Inc.). Large-scale 10× reactions (300 μl) were prepared using DKY6281 background vacuoles (60 μg) and incubated at 27 °C for 60 min. Neutral lipids were first extracted from vacuoles by the addition of 3 ml of MeOH/$CHCl_3$ (2:1) and vortexing three times over 10 min at room temperature. Insoluble lipids were collected by centrifugation (1500 × *g*, 5 min), and the supernatant was discarded. Next, acidic lipids were extracted by the addition of 2.25 ml of MeOH, $CHCl_3$, and 12 M HCl (80:40:1) and vortexing four times over 15 min at room temperature. Insoluble lipids were collected by centrifugation, and the supernatant was transferred to a 15-ml centrifuge tube. The acidic lipid fraction was treated with 0.75 ml of $CHCl_3$ and 1.35 ml of 0.1 M HCl, vortexed, and phase-separated by centrifugation as described above. The lower organic phase was collected, transferred into a new 1.5-ml microcentrifuge tube, and dried down in a SpeedVac system for 1 h. The dried lipids were resuspended in 190 μl of PBS/Tween 20 with 3% protein stabilizer. Samples were vortexed for 1 min and centrifuged prior to use in ELISA. ELISA was performed according to the manufacturer's instructions.

trans-SNARE Complex Assay—Analysis of *trans*-SNARE complex formation was performed as described previously (7, 26, 27). Complex formation was compared in reactions containing vacuoles from RFY33 and RFY55 relative to vacuoles from BJ3505 CBP-Vam3p *nyv1*Δ and DKY6281. The *trans*-SNARE assays were performed using 16× large-scale reactions (480 μl) containing 48 μg of vacuoles each from BJ3505 CBP-Vam3p *nyv1*Δ and DKY6281 backgrounds. Reactions were incubated at 27 °C for 60 min and then placed on ice for 5 min prior to collecting 30 μl from each sample to test Pho8p activity. The remaining samples were centrifuged (13,000 × *g*, 15 min, 4 °C), and the supernatants were discarded. Vacuole pellets were overlaid with 200 μl of ice-cold solubilization buffer (20 mM Tris-Cl (pH 7.5), 150 mM NaCl, 1 mM $MgCl_2$ 0.5% Nonidet P-40 alternative, and 10% glycerol) with protease inhibitors (0.46 μg/ml leupeptin, 3.5 μg/ml pepstatin, 2.4 μg/ml Pefabloc SC, and 1 mM PMSF) and resuspended. Solubilization buffer was added to a final volume of 600 μl, and extracts were mixed for 20 min at 4 °C with nutating, followed by centrifugation (16,000 × *g*, 20 min, 4 °C) to remove detergent-insoluble material. Supernatants were transferred to new tubes, and 10% of the extract was removed for input samples. The extracts were brought to 2 mM $CaCl_2$ and incubated with 50 μl of equilibrated calmodulin-Sepharose 4B (GE Healthcare) at 4 °C for 12 h with nutating. Beads were collected by centrifugation (4000 × *g*, 2 min, 4 °C) and washed with solubilization buffer, followed by bead sedimentation. Bound proteins were eluted with SDS sample buffer containing 5 mM EGTA and heated at 95 °C for 5 min. The samples were used for SDS-PAGE analysis and immunoblotting.

Vacuoles were isolated from yeast harboring *YCF1* fused to a tandem affinity purification (TAP) tag. Protein complexes were isolated as described (28) with some modification. 10% of the extract was removed for input samples. For each strain, 1 ml of vacuoles at 1 mg/ml was incubated with 500 μl of IgG-Sepharose 6 Fast Flow (GE Healthcare) equilibrated with Nonidet P-40 alternative buffer (15 mM Na_2HPO_4, 10 mM NaH_2PO_4-H_2O, 1.0% Nonidet P-40 alternative, 150 mM NaCl, and 2 mM EDTA) containing a protease inhibitor mixture (1 mM PMSF, 0.46 μg/ml leupeptin, and 3.5 μg/ml pepstatin) and incubated at 4 °C for 2 h with nutating. After incubation, the beads were washed twice with 10 ml of buffer containing 25 mM Tris-Cl (pH 8.0), 300 mM NaCl, and 0.1% Nonidet P-40 alternative and once with buffer containing 25 mM Tris-Cl (pH 8.0), 150 mM NaCl, and 0.1% Nonidet P-40 alternative. Next, the beads were washed with 10 ml of tobacco etch virus protease buffer (25 mM Tris-Cl (pH 8.0), 150 mM NaCl, 0.1% Nonidet P-40 alternative, and 0.5 mM EDTA), resuspended with 1 ml of tobacco etch

virus protease buffer containing 5 μg of tobacco etch virus protease, and incubated at 4 °C for 2 h with nutating. Released proteins were collected, mixed 1:1 with calmodulin binding buffer (25 mM Tris-Cl (pH 8.0), 150 mM NaCl, 1 mM magnesium acetate, 1 mM imidazole, 2 mM $CaCl_2$, and 10 mM β-mercaptoethanol), incubated with 300 μl of calmodulin-Sepharose 4B equilibrated in calmodulin binding buffer, and incubated for 1 h at 4 °C with nutating. Protein-bound beads were washed twice with calmodulin binding buffer with 0.1% Nonidet P-40 alternative and three times with calmodulin binding buffer containing 0.02% Nonidet P-40 alternative. Protein complexes were eluted with 1 ml of calmodulin elution buffer (25 mM Tris-Cl (pH 8.0), 150 mM NaCl, 0.02% Nonidet P-40 alternative, 1 mM magnesium acetate, 1 mM imidazole, 20 mM EGTA, and 10 mM β-mercaptoethanol) into a siliconized microcentrifuge tube. Eluted proteins were TCA-precipitated. Dried proteins were solubilized with SDS-PAGE buffer and processed for immunoblotting.

Ca^{2+} Efflux Assay—Vacuole lumen Ca^{2+} efflux was measured as described (11). Fusion reactions (60 μl) contained 20 μg of vacuoles isolated from BJ3505 backgrounds, fusion reaction buffer with 10 μM CoA, 283 nM inhibitor of protease B (IB_2), and the fluorescent Ca^{2+} probe Fluo-4 dextran (200 μM; Invitrogen). Reaction mixtures were transferred to a black half-volume 96-well flat-bottom plate with a nonbinding surface. An ATP-regenerating system or buffer was added, and reactions were incubated at 27 °C while monitoring Fluo-4 fluorescence.

RESULTS

ABCC Transporter Localization to Vacuoles—The yeast vacuole harbors multiple ABCC transporters, including Ycf1p, Bpt1p, Vmr1p, and Nft1p. Here, we compared the relative abundance of each transporter in our yeast tester strains by expressing GFP fusions. We also examined the distribution of the putative ABCC transporter YOL075c. Yeast cells were grown with the vital dye FM 4-64, which is endocytosed and accumulates on the vacuole membrane. Colocalization analysis showed that Ycf1p-GFP and Bpt1p-GFP were highly enriched on the vacuole relative to the other transporters tested (Fig. 1). Although Vmr1p-GFP, Nft1p-GFP, and YOL075c-GFP were detected on vacuoles, these proteins were also present in other membrane pools, yielding a hazy cytoplasm.

YCF1 and BPT1 Deletions Attenuate Vacuole Fusion—Although ABCC transporters function primarily in detoxification of yeast cytoplasm, new studies have shown that some family members perform additional functions. For example, Ybt1p regulates calcium homeostasis and vacuole fusion and has been shown to translocate phosphatidylcholine to aid in choline recycling (11, 12, 29). Others have shown that Ycf1p physically interacts with Fab1p, a PI3P 5-kinase that modifies PI3P, a lipid that is essential for vacuole fusion (3, 9, 18). Here, we examined the possible role of ABCC transporters in the fusion process. *YCF1*, *BPT1*, *VMR1*, *NFT1*, and *YOL075C* were deleted from our fusion tester strains and examined for abnormalities in the fusion pathway. These experiments showed that *ycf1*Δ and *bpt1*Δ vacuoles were attenuated for fusion by 30–40% relative to wild-type parent strains (Fig. 2, *A* and *B*). Interestingly, *vmr1*Δ, *nft1*Δ, and *yol075c*Δ vacuoles showed no defects in vacuole fusion (data not shown). This suggests that the effects of deleting *YCF1* and *BPT1* were specific to functions of the individual proteins and not to general characteristics of ABCC family members. To determine whether the effects of deleting *YCF1* and *BPT1* were additive, we generated double deletion strains (*ycf1*Δ/*bpt1*Δ) and examined fusion. We found that deletion of both genes did not inhibit fusion further (Fig. 2*C*), suggesting that there was some redundancy in their function. Previously, we found that deletion of the ABCC transporter *YBT1* stimulated fusion up to 50% above wild-type fusion (11). To examine whether the absence of Ybt1p would compensate for the fusion defect seen with *ycf1*Δ/*bpt1*Δ vacuoles, we produced triple deletion fusion tester strains (*ycf1*Δ/*bpt1*Δ/*ybt1*Δ). We found the triple deletion restored fusion to wild-type levels. This suggests that the fusion defect seen in *ycf1*Δ/*bpt1*Δ vacuoles was not due to irreversible deleterious effects and that the two effects offset each other. To verify that the inhibited fusion was not due to inhibition of the Pho8p reporter system, we also examined the effects of deleting *YCF1* and *BPT1* using a nonenzymatic reporter system. Here, vacuoles were labeled with Rh-PE at self-quenching levels (27). Labeled vacuoles were incubated with an excess of unlabeled vacuoles, and fusion was measured by the dilution and dequenching of Rh-PE. Fig. 2*E* shows that *ycf1*Δ/*bpt1*Δ vacuoles were inhibited for fusion by fluorescence dequenching at levels similar to those shown in Fig. 2*C*. Because the double deletion did not further reduce fusion, the remainder of the study was performed with *YCF1* single deletion strains. Attenuated fusion is often linked with vacuole fragmentation; thus, we examined the vacuole morphology of *ycf1*Δ cells as described above. Although *ycf1*Δ vacuoles were attenuated for fusion, we did not observe a defect in vacuole morphology relative to the wild-type parent strain (Fig. 2*F*). We attribute the lack of a fragmentation defect to the

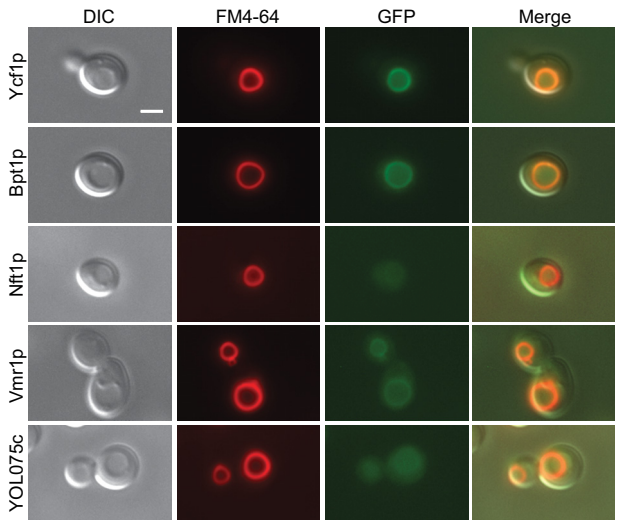

FIGURE 1. **Ycf1-GFP is localized to the vacuole.** Wild-type yeast cells harboring Ycf1p-GFP, Bpt1p-GFP, Nft1p-GFP, Vmr1p-GFP, or YOL075c-GFP were incubated with 5 μM FM 4-64 to label vacuoles. Cells were washed with PBS and grown for 1 h in label-free YPD medium to chase the dye into the vacuole. Cells were washed with PBS and mounted for microscopy. GFP images were acquired using a 38 HE GFP shift-free filter set, and FM 4-64 images were acquired using a 43 HE Cy3 shift-free filter set. Cells were photographed using differential interference contrast (*DIC*). Images were merged using Photoshop. *Scale bar* = 4 μm.

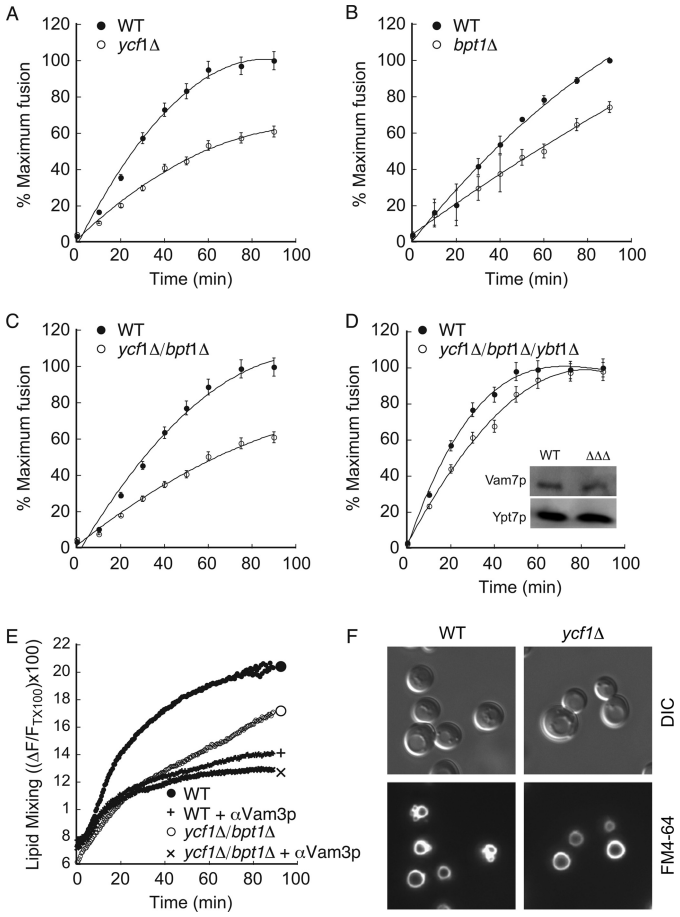

FIGURE 2. **Deletion of *YCF1 and BPT1* attenuates vacuole fusion.** Vacuoles were harvested from WT, *ycf1*Δ (*A*), *bpt1*Δ (*B*), *ycf1*Δ/*bpt1*Δ (C), and *ycf1*Δ/*bpt1*Δ/*ypt1*Δ (*D*) yeast and tested for fusion activity. Standard fusion reactions used equal amounts of reporter (*PHO8 pep4*Δ) and effector (*pho8*Δ *PEP4*) vacuoles. *Error bars* represent S.E. ($n = 3$). *D*, *inset*, vacuoles were isolated from WT and *ycf1*Δ/*bpt1*Δ/*ybt1*Δ strains and examined for Vam7p content. Blotting for Ypt7p served as a loading control. *E*, lipid mixing assays measuring fusion were performed by labeling isolated vacuoles with Rh-PE. Labeled vacuoles were incubated with an 8-fold excess of unlabeled vacuoles, and dequenching was measured using a fluorescence plate reader. *F*, WT and *ycf1*Δ yeast cells were stained with FM 4-64, and vacuole morphology was analyzed by fluorescence microscopy. *DIC*, differential interference contrast.

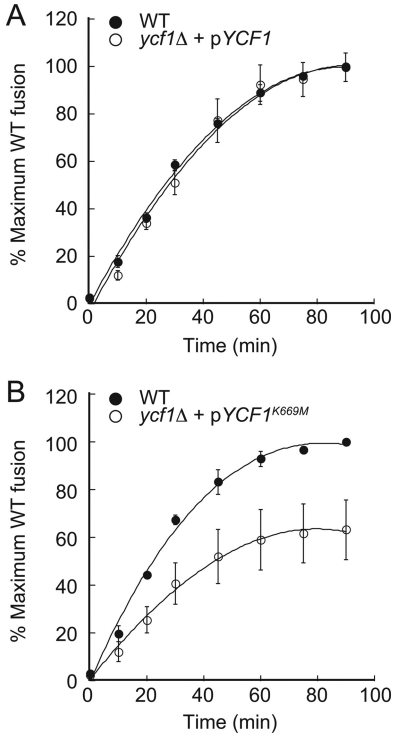

FIGURE 3. **ATPase activity of Ycf1p is required to support vacuole fusion.** *ycf1*Δ cells were complemented with plasmid-expressed wild-type Ycf1p (*A*) or mutant Ycf1p^{K669M} (*B*). Vacuoles were isolated from these strains and tested for fusion activity. *Error bars* represent S.E. ($n = 3$).

redundant functions of ABCC transporters and to the supply of the soluble SNARE Vam7p in the cytoplasm, which will be elucidated below.

Ycf1p-supported Fusion Requires ATPase Activity—To determine whether the role of Ycf1p in vacuole fusion is dependent on its transporter activity, we complemented *ycf1*Δ cells with plasmid-expressed wild-type Ycf1p or mutant Ycf1p^{K669M}. The point mutation was in the Walker A motif of the first nucleotide-binding domain. The conserved lysine is required for ATP hydrolysis and growth in the presence of cadmium (15). Complementation of *ycf1*Δ strains with wild-type p*YCF1* fully rescued fusion (Fig. 3*A*), indicating that the inhibition was directly due to the absence of Ycf1p. However, when *ycf1*Δ strains were complemented with the ATPase-deficient mutant p*YCF1*^{K669M}, fusion remained attenuated (Fig. 3*B*), suggesting that the transport function of Ycf1p was important for the regulation of fusion. It was previously shown that Ycf1p^{K669M} was properly trafficked to the vacuole (15), indicating that the inability of Ycf1p^{K669M} to rescue fusion was linked to its ATPase activity and not a sorting defect.

Ycf1p Regulates Vam7p Recruitment to Vacuoles—Changes in vacuole fusion can be due to alterations in the trafficking of fusion regulators to the vacuole; thus, we examined the protein profile of *ycf1*Δ vacuoles. Fig. 4*A* shows the levels of SNAREs (Vam3p, Vam7p, Vti1p, and Nyv1p), their chaperones Sec18p and Sec17p, HOPS subunits (Vps11p, Vps33p, and Vps41), Ypt7p, and other fusion regulators in wild-type and *ycf1*Δ vacuoles. Most proteins were equally abundant on wild-type and *ycf1*Δ vacuoles, with the prominent exception of the soluble SNARE Vam7p. Mutant *ycf1*Δ vacuoles contained 30–40% less Vam7p relative to wild-type vacuoles (Fig. 4*B*), suggesting that the defect in fusion was due in part to depletion of a SNARE protein. The Levels of Pho8p and Pep4p were also analyzed, and there were no significant changes in either component of the reporter system, further indicating that the attenuated fusion of *ycf1*Δ vacuoles was due to changes in the fusion machinery and not Pho8p activation. To determine whether the reduction in vacuole-associated Vam7p was due to defective recruitment or degradation of the protein, we examined Vam7p levels in whole cell lysates. There was no observable difference in Vam7p levels between WT and *ycf1*Δ cells (Fig. 4*C*), indicating that mutant vacuoles were unable to recruit sufficient Vam7p to support fusion. Actin levels were probed as a loading control.

To further examine the distribution of Vam7p in WT and *ycf1*Δ cells, we performed cellular fractionation as described (10). Vam7p distribution was examined by immunoblotting (Fig. 5*A*). We observed an increase of Vam7p in the cytosolic fraction of *ycf1*Δ relative to WT cytosol. We also probed for

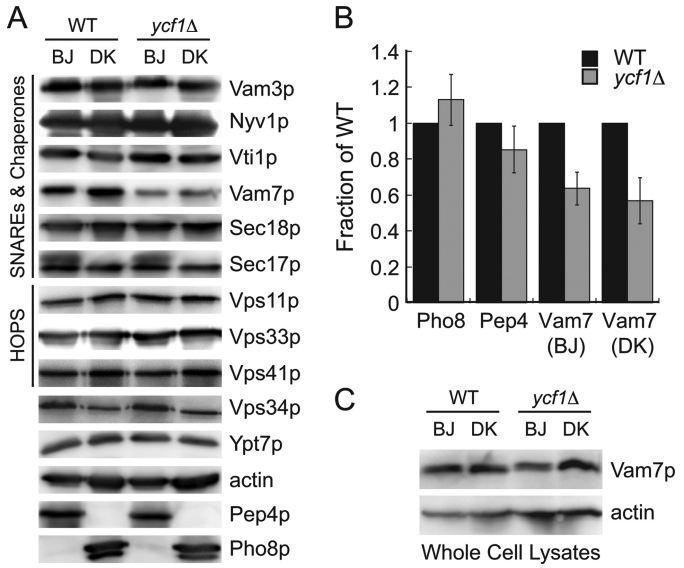

FIGURE 4. **Vam7p depletion on *ycf1*Δ vacuoles regulates vacuole fusion.** *A*, analysis of core fusion components. Vacuoles were isolated from WT and *ycf1*Δ BJ3505 (*BJ*) and DKY6281 (*DK*) strains. Vacuoles (5 μg/protein) were mixed with 2× SDS loading buffer, separated by SDS-PAGE, and transferred to nitrocellulose. Immunoblotting was performed using the indicated antibodies, and bands were detected using enhanced chemifluorescence. *B*, quantitation of Vam7p, Pho8p, and Pep4p levels on WT and *ycf1*Δ vacuoles. *C*, Western blots of Vam7p and actin in whole cell lysates of WT and *ycf1*Δ yeast. *BJ*, BJ3505; *DK*, DKY6281.

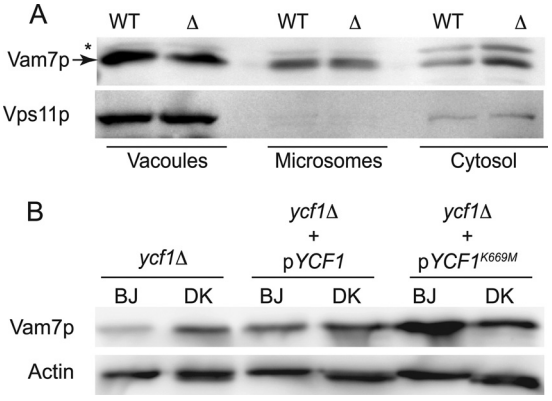

FIGURE 5. **YCF1 deletion and Vam7p distribution.** *A*, WT and *ycf1*Δ cells were fractionated into cytosol, microsomes, and vacuoles (7, 10). The distribution of Vam7p was examined by immunoblotting. Antibody against Vps11p was used to detect vacuolar contents and served as a loading control. *B*, vacuoles were isolated from *ycf1*Δ cells or *ycf1*Δ cells complemented with plasmids to express wild-type Ycf1p or Ycf1p^{K669M}. Vacuoles were probed for Vam7p content by immunoblotting. Blotting for actin served as a loading control.

Vps11p as a marker for vacuoles and as a loading control. These data are in accord with the idea that Ycf1p plays a role in the recruitment of Vam7p. However, it is unclear whether Vam7p recruitment was direct or indirect.

In this study, we determined that deleting *YBT1* in *ycf1*Δ/*bpt1*Δ cells restored fusion to WT levels. Because of the role of Ycf1p in Vam7p recruitment, we examined Vam7p recruitment to *ycf1*Δ/*bpt1*Δ/*ybt1*Δ vacuoles. Vacuoles were isolated from WT and *ycf1*Δ/*bpt1*Δ/*ybt1*Δ cells and immunoblotted for Vam7p and Ypt7p. We found that *ycf1*Δ/*bpt1*Δ/*ybt1*Δ cells harbored similar levels of Vam7p relative to WT vacuoles (Fig. 2*D*, *inset*). Ypt7p levels were measured as a loading control. These data suggest that the triple deletion mimicked the conditions necessary for Vam7p recruitment.

The role of Ycf1p in fusion was not limited to its physical presence and potential interactions with the fusion machinery. This was demonstrated by the inability of Ycf1p^{K669M} to support fusion (Fig. 3*B*). When vacuoles from Ycf1p^{K669M} yeast were immunoblotted for Vam7p, we found that these vacuoles contained elevated levels of Vam7p relative to *ycf1*Δ vacuoles or those from *ycf1*Δ yeast complemented with WT Ycf1p (Fig. 5*B*). Actin levels were measured as a loading control. This suggests that Ycf1p-dependent recruitment of Vam7p was insufficient to restore fusion. Furthermore, this indicates that the ATPase-dependent transport activity of Ycf1p played a role in regulating fusion.

*Exogenous Vam7p Restores Fusion of ycf1*Δ *Vacuoles*—Vam7p directly interacts with the HOPS complex as well as other SNAREs (30, 31); however, the levels of these proteins were not affected on *ycf1*Δ vacuoles. Vam7p also interacts with the lipid PI3P (32), which is made on the vacuole during fusion by the phosphatidylinositol kinase Vps34p (33), yet the levels of this lipid kinase were also unaffected on mutant vacuoles. However, these data do not show whether the association of Vam7p with its binding partners was affected on mutant vacuoles. To test whether the simple lack of Vam7p affected *ycf1*Δ vacuole fusion, we added exogenous recombinant GST-Vam7p to fusion reactions containing either wild-type or *ycf1*Δ vacuoles. We found that the direct addition of Vam7p during the fusion reaction rescued *ycf1*Δ vacuole fusion to wild-type levels (Fig. 6*A*). This indicates that Vam7p could function with its binding partners during fusion and that the defect in *ycf1*Δ vacuole fusion was due to the inability to recruit wild-type levels of Vam7p. We also observed that high levels of Vam7p reduced fusion. This is consistent with previous studies showing a biphasic curve of the effects of Vam7p on fusion (20, 21).

Thus far, we have found that *ycf1*Δ vacuoles harbored reduced levels of Vam7p and that the exogenous addition of this SNARE rescued the fusion phenotype. Accordingly, we posited that the levels of *trans*-SNARE complexes might also be reduced on *ycf1*Δ vacuoles. Here, we used a well characterized assay that measures *bona fide trans*-SNARE complex formation. This was performed using two distinct vacuole populations. One set of vacuoles was isolated from a *nyv1*Δ deletion strain that harbors Vam3p containing an internal calmodulin-binding peptide (CBP-Vam3p). These vacuoles were mixed with WT vacuoles (*NYV1 VAM3*). Thus, the isolable *trans*-SNARE complexes formed between CBP-Vam3p and Nyv1p were generated from the docking of separate organelles. In our experiments, we found that *ycf1*Δ vacuoles formed significantly less *trans*-SNARE complexes relative to those containing Ycf1p. The addition of exogenous Vam7p (50 nM) resulted in an increase in Nyv1p-CBP-Vam3p complex formation for both sets of vacuoles (Fig. 6, *B* and *C*). This indicated that the increase in fusion shown in Fig. 6*A* was due to increased SNARE complex formation. The MARCKS effector domain was used as an inhibitor of fusion (7). Quantitation of three experiments showed that the addition of recombinant Vam7p had a positive effect on SNARE complex formation on both WT and *ycf1*Δ vacuoles (Fig. 6*C*).

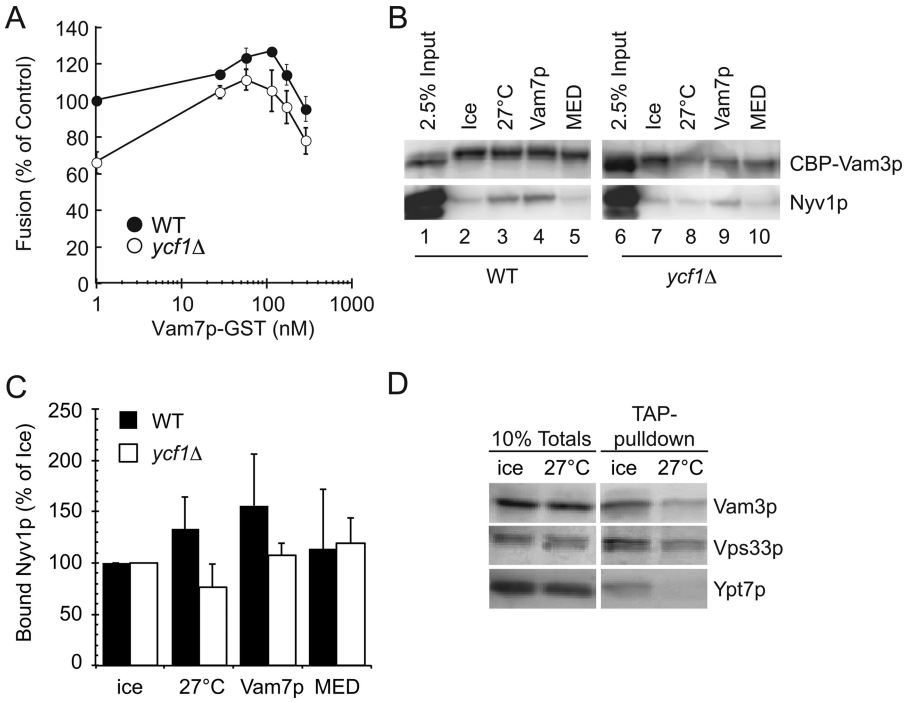

FIGURE 6. **Ycf1p interacts with the fusion machinery.** *A*, fusion reactions containing WT or *ycf1*Δ vacuoles were incubated with recombinant GST-Vam7p and tested for fusion as described in Fig. 2. *Error bars* represent S.E. ($n = 3$). *B*, *trans*-SNARE complexes were isolated from WT and *ycf1*Δ vacuoles as described under Experimental Procedures." Reactions were incubated at 4 or 27 °C and treated with buffer, 50 nM recombinant Vam7p, or the MARCKS effector domain (MED) as indicated. Immunoblotting was performed to probe for Vam3p and Nyv1p. *C*, quantitation of *trans*-SNARE complex formation for *B*. Data represent means ± S.E. ($n = 3$). *D*, Ycf1p-TAP complexes were isolated as described under "Experimental Procedures." Reactions were incubated for 60 min at 27 °C or on ice and then processed for Ycf1p-TAP isolation. Protein complexes were examined by immunoblotting using antibodies against Vps33p, Vam3p, and Ypt7p.

Ycf1p Interacts with the Fusion Machinery—The reduction of Vam7p in *ycf1*Δ vacuoles led us to hypothesize that Ycf1p may directly interact with the fusion machinery. To test this notion, we used vacuoles harboring Ycf1p-TAP to isolate factors physically interacting with Ycf1p. We found that Ycf1p-TAP co-purified with the Vps33p subunit of HOPS as well as Vam3p (Fig. 6*D*). These results do not indicate, however, which protein was in direct contact with Ycf1p-TAP. We also observed a weak interaction with Ypt7p when reactions remained on ice. The interaction was lost when vacuoles were brought up to 27 °C, suggesting that the interaction was nonspecific. We also loaded 10% of the total extracts as a control for starting material.

*Exogenous Vam7p Restores Ca^{2+} Efflux in ycf1*Δ *Vacuoles*—Thus far, we have observed that the fusion defect in *ycf1*Δ vacuoles was due in part by the exclusion of Vam7p from the vacuole, which could lead to a reduction in *trans*-SNARE pairing. Because the formation of *trans*-SNARE complexes triggers the release of lumenal Ca^{2+} stores from the vacuole prior to fusion (34, 35), we next determined if the reduced level of *trans*-SNARE complexes seen using *ycf1*Δ vacuoles correlated with a decrease in Ca^{2+} efflux. Fusion reactions containing wild-type or *ycf1*Δ vacuoles were incubated with standard fusion reaction components in the presence of the fluorescent calcium indicator Fluo-4 dextran (11). Reactions were started by the addition of buffer or an ATP-regenerating system. In the absence of ATP, Fluo-4 fluorescence remained stable, whereas fluorescence decreased in the presence of ATP during the first 20 min of the reactions (Fig. 7*A*), indicating that Ca^{2+} was taken up by the vacuoles. We inhibited selected reactions with Gyp1–46p to inhibit Ypt7p-dependent docking as a negative control. Gyp1–46p-inhibited reactions showed continued Fluo-4 fluorescence until a base line was reached. Interestingly, the initial uptake of Ca^{2+} was measurably greater in *ycf1*Δ reactions relative to wild-type reactions. This could be attributed to differences in the relative amounts of Vam7p and *trans*-SNARE complexes on mutant vacuoles. After 15–20 min of incubation, the uninhibited reactions released Ca^{2+} that correlated with the formation of *trans*-SNARE complexes. Reactions containing *ycf1*Δ vacuoles released Ca^{2+} at the same time as those containing wild-type vacuoles, but the external concentration of cations did not reach wild-type levels. Again, this was likely due to the reduced number of *trans*-SNARE complexes present on *ycf1*Δ vacuoles. It should also be noted that there was no difference in the net amount of released Ca^{2+} in mutant reactions. To determine whether the levels of Vam7p were linked to the changes in Ca^{2+}, we performed experiments in the presence or absence of exogenous Vam7p. We found that the addition of supplemental Vam7p to reactions eliminated the differences in Ca^{2+} efflux between *ycf1*Δ and wild-type vacuoles (Fig. 7*B*). This was consistent with the effect of exogenous Vam7p on the fusion of *ycf1*Δ vacuoles in Fig. 6 and suggests that the primary defect in these vacuoles was the defective recruitment of Vam7p.

Ycf1p Regulates PI3P Accumulation at Vertex Microdomains—In addition to binding HOPS and SNAREs, Vam7p binds the regulatory lipid PI3P. This lipid is required for fusion in part by its function in the assembly of vertex microdomains as well as the direct recruitment of Vam7p (3, 32). Although the lipid kinase Vps34p was present on *ycf1*Δ vacuoles, it remained possible that PI3P levels were insufficient to recruit Vam7p to the

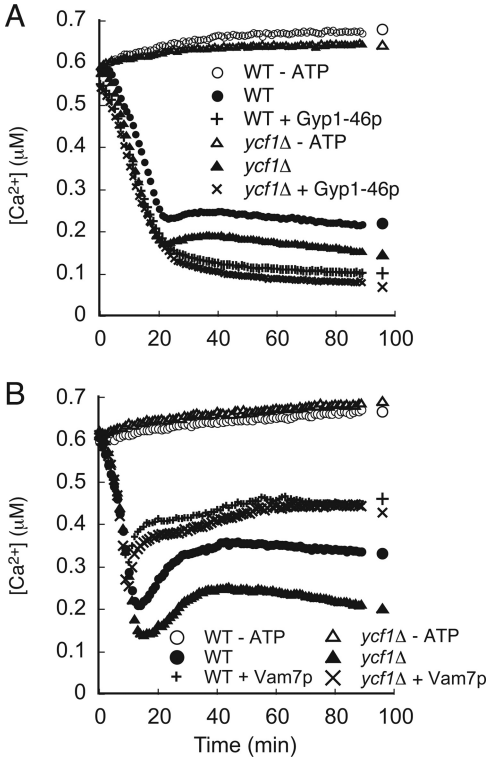

FIGURE 7. **Exogenous Vam7p rescues the defective Ca^{2+} efflux of *ycf1*Δ vacuoles.** Vacuoles were harvested from WT BJ3505 and RFY32 (*ycf1*Δ). Fusion reactions (2×) were prepared and contained 20 μg of either WT or *ycf1*Δ vacuoles and 200 μM Fluo-4 dextran. Immediately after the addition of ATP or PS buffer, reactions were incubated at 27 °C, and fluorescence was measured for 90 min. *A*, reactions were treated with buffer or Gyp1–56. *B*, reactions were treated with buffer or GST-Vam7p. Representative experiments of three repeats are shown.

vacuole. To examine the levels and distribution of PI3P on wild-type and *ycf1*Δ vacuoles, we used ratiometric fluorescence microscopy and quantitative ELISAs. To track PI3P accumulation in vertex microdomains, we incubated reactions containing either wild-type or *ycf1*Δ vacuoles with the specific PI3P ligand FYVE domain (19). The FYVE domain was conjugated with the fluorophore Cy5. After incubation, the docking reactions were placed on ice and stained with MDY-64 to label the limiting vacuole membrane (3, 4). We found that *ycf1*Δ vacuoles contained elevated levels of PI3P at the vertices of docked vacuoles relative to wild-type vacuoles (Fig. 8*A*). Cy5-FYVE accumulation at vertices relative to the outer edge of membranes was measured as the ratio of Cy5-FYVE to MDY-64. Vertex and outer edge ratios were plotted on cumulative distribution plots. The right shift of the *ycf1*Δ vertex curve relative to the wild-type vertex curve indicated that there was more PI3P at the vertices of *ycf1*Δ vacuoles. Fig. 8*B* shows the geometric means and 95% confidence intervals of the curves in Fig. 8*A* and shows that the enhanced vertex enrichment of PI3P on *ycf1*Δ vacuoles was statistically significant ($p < 0.0001$). To determine whether the difference in PI3P distribution was due to absolute changes in lipid concentrations or enhanced microdomain formation, we used a quantitative ELISA to measure the total levels of PI3P in solubilized wild-type and *ycf1*Δ vacuoles. Fig. 8*C* shows that the total levels of PI3P in *ycf1*Δ vacuoles were not significantly different from those in wild-type vacuoles. Taken together, these data suggest that PI3P accumulated at vertices with more efficiency in the absence of Ycf1p. It was also possible that the absence of Vam7p on *ycf1*Δ vacuoles resulted in more PI3P available for Cy5-FYVE staining.

To examine the distribution of PI3P *in vivo*, WT and *ycf1*Δ cells were transformed with plasmid-encoding GFP-FYVE (36). Cells were incubated with the vital dye FM 4-64 to label vacuoles as described previously (37), and cells were examined by fluorescence microscopy. We found that both WT and *ycf1*Δ vacuoles were similarly labeled with GFP-FYVE (Fig. 8*D*). This was in accord with the quantitative ELISA.

DISCUSSION

Ycf1p regulates the transport of cadmium, mercury, and other toxins into the vacuole lumen to detoxify the cytoplasm (14, 38, 39). However, a role for Ycf1p in the regulation of fusion had not been directly examined. Interestingly, an iMYTH (integrated split-ubiquitin membrane yeast two-hybrid) analysis showed that Ycf1p physically interacts with the PI3P 5-kinase Fab1p, which uses PI3P to produce $PI(3,5)P_2$. It also interacts with the Rho1p nucleotide exchange factor, Tus1p (18). Others have found that Ycf1p physically interacts directly with Rho1p, a GTPase associated with actin dynamics (40). Because Rho1p (41), actin (42, 43), and PI3P (3) play important roles in vacuole fusion, we examined the effect of deleting *YCF1* and other ABCC transporters on vacuole fusion. We found that *ycf1*Δ and *bpt1*Δ vacuoles were each attenuated for fusion, yet the double deletion did not exhibit additive effects. The defect in fusion was relieved by also deleting *YBT1*, an ABCC transporter previously reported to negatively regulate vacuole fusion (11). The mechanism(s) for the rescued fusion remain unclear and will be further explored in future studies. The rest of this study focused on the effect of deleting *YCF1* alone. We found that the attenuated fusion seen with *ycf1*Δ vacuoles was due to the diminished recruitment of Vam7p. The defect in fusion was rescued by the addition of recombinant Vam7p. The exclusion of Vam7p from *ycf1*Δ vacuoles was not due to the lack of known binding partners (including SNAREs, HOPS, and the regulatory lipid PI3P), which were all at wild-type levels. Moreover, exogenous Vam7p readily associated with the vacuoles to trigger fusion, suggesting that neither Vam7p-protein nor Vam7p-PI3P interactions were adversely affected by the lack of Ycf1p.

Of the published iMYTH results, the interaction between Ycf1p and Fab1p stands out with respect to vacuole fusion. PI3P is generated during fusion (33) by the phosphatidylinositol kinase Vps34p (9), and the absence or sequestering of PI3P has severe negative effects on the fusion machinery. This lipid is required for the recruitment of Vam7p as well as the formation of membrane raft domains and the interactions between SNAREs and HOPS (3, 44, 45). PI3P levels can be reduced through the phosphatase activity of Ymr1p or the kinase activity of Fab1p (46, 47), although it remains unknown whether either Ymr1p or Fab1p functions during vacuole homotypic fusion. Regarding vacuole homeostasis, the importance of $PI(3,5)P_2$ has been linked to acidification, trafficking to the vacuole, and response to hypertonic shock (48–50). However, the role of $PI(3,5)P_2$ in vacuole fusion remains unclear. Previous work has shown that deletion of *FAB1* does not affect vacuole

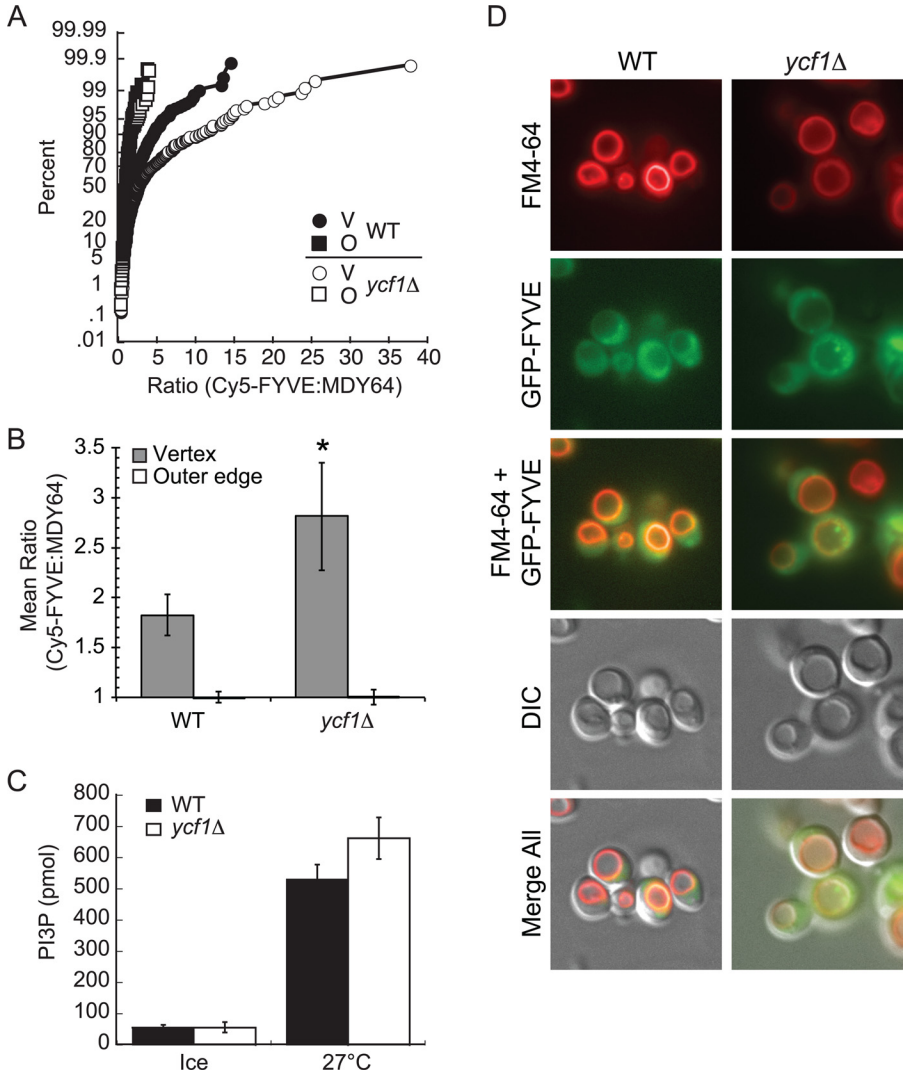

FIGURE 8. **PI3P levels are increased at the vertices of docked *ycf1*Δ vacuoles.** *A*, cumulative distribution plots show the percentile values of Cy5-FYVE/MDY-64 ratios for each vertex (*V*) and outer edge (*O*). Each curve is compiled from at least 10 vacuole clusters, where the maximum pixel intensity was determined for every vertex and midpoint of the outer edge membrane. Pixel intensities were measured in both fluorescence channels at each subdomain and are expressed as a ratio of Cy5-FYVE to MDY-64. Outer edge ratios were normalized to a value of 1, and the enrichment of Cy5-FYVE at vertices is expressed relative to outer edge intensities. Each ratio in a data set is ordered and plotted *versus* the percentile rank of the values. *B*, geometric means with their 95% confidence intervals for the data in *A*. *, $p < 0.05$. *C*, quantitative ELISA analysis of PI3P levels in WT and *ycf1*Δ vacuole fusion reactions after 60 min of incubation at 27 °C. *Error bars* represent S.E. ($n = 3$). *D*, WT and *ycf1*Δ cells were transformed with plasmid to express GFP-FYVE. Cells were treated with FM 4-64 to label vacuoles, and cells were examined by fluorescence microscopy. *DIC*, differential interference contrast.

fusion under isotonic conditions (51), suggesting that formation of $PI(3,5)P_2$ is not essential for fusion to occur. Nevertheless, a regulatory role was not ruled out for the lipid. In this study, we found that PI3P levels were similar in WT and *ycf1*Δ vacuoles, suggesting that any Ycf1p-dependent Fab1p activity had no effect on the steady-state levels of PI3P. Although the levels of PI3P did not change between the WT and *ycf1*Δ strains, we did observe a marked increase in PI3P accumulation at the vertices of docked vacuoles. Although the mechanism for the altered distribution remains unclear, we are able to propose a link between the PI3P localization and the Ycf1p-Tus1p interaction. Tus1p is the nucleotide exchange factor for Rho1p, a GTPase involved in actin remodeling and vacuole fusion (41, 52). Moreover, Ycf1p directly interacts with Rho1p (40). Because actin remodeling is essential for vacuole fusion at different stages of the reaction, we can theorize that in the absence of Ycf1p, Rho1p might be inactive, resulting in a reduction in actin polymerization on vacuoles. Importantly, we previously reported a link between PI3P localization to vertices and the state of actin polymerization (3). When actin was depolymerized by latrunculin B, vertex-localized PI3P levels were dramatically increased on docked vacuoles. In contrast, when F-actin was stabilized by jasplakinolide, PI3P enrichment was completely inhibited. Together, these results suggest that Ycf1p may play a role in the state of actin polymerization on vacuoles and the subsequent lateral mobilization of PI3P on docked vacuoles.

In this study, we also found that the ATPase activity of Ycf1p was important for vacuole fusion. A point mutation that substituted the conserved Lys with Met in the Walker A box motif of the first nucleotide-binding domain prevented the complementation of the *ycf1*Δ fusion defect. Although physical interactions between Ycf1p and trafficking proteins have been doc-

umented by iMYTH, the interactions were independent of ATPase activity and were not in the context of the vacuole. Because the addition of recombinant Vam7p rescued *ycf1*Δ vacuole fusion, we posit that the direct transport activity of Ycf1p is not related to Vam7p recruitment to the vacuole membrane. One possible mechanism for the link between these two proteins is the putative "flippase" activity of Ycf1p and other ABCC transporters. Although flippase activity has not been reported for Ycf1p, its paralog Ybt1p has been reported to translocate (or flip) phosphatidylcholine from the outer-to-inner leaflets of the vacuole membrane (12). Thus, it is not unlikely that Ycf1p may also function as a lipid translocation enzyme for other lipids. This is important because Vam7p binding to the vacuole is regulated by the composition of the outer leaflet vertex microdomains of vacuoles (3), where it was shown that disruption of the vertex microdomain by binding or modifying various lipids other than PI3P inhibited the binding of Vam7p to vacuoles. Therefore, if Ycf1p modifies the lipid composition of the vacuole outer leaflet, inactivating its ATPase-dependent translocation activity could alter the steady-state association of Vam7p. Our unpublished preliminary studies have indicated that vacuoles flip Rh-PE.[4] However, this activity was not dependent on Ycf1p.

Importantly, we found that Ycf1p formed stable complexes with the fusion machinery. Ycf1p-TAP was co-purified with SNAREs and the HOPS complex, suggesting that Ycf1p may play a role in regulating the core fusion machinery as evident by the defective Vam7p recruitment to *ycf1*Δ vacuoles. There is a growing body of work that links various ABC transporters to membrane trafficking pathways. For instance, the ABCC mammalian chloride channel cystic fibrosis transmembrane conductance regulator (CFTR) interacts with the SNARE motif of syntaxin 1a at the plasma membrane, and disruption of the interaction inhibits CFTR-mediated currents (53). CFTR also interacts with EBP50 (ERM-binding protein 50), a protein that bridges CFTR to the actin cytoskeleton (54). Others have shown that ABCA1 interacts with syntaxin 13 and flotillin-1 in monocytes (55). In addition, we found that the ABCC protein Ybt1p is linked to the regulation of vacuole fusion through affecting the transport of Ca^{2+} across the membrane (11). Although the regulatory mechanisms driven by these interactions remain to be elucidated, it is clear that ABC transporters play important roles in membrane trafficking.

Acknowledgments—We thank Drs. William Wickner and W. Scott Moye-Rowley for generous gifts of antisera and plasmids. We also thank members of the Fratti laboratory for critical reading of the manuscript.

REFERENCES

1. Jahn, R., and Südhof, T. C. (1999) Membrane fusion and exocytosis. *Annu. Rev. Biochem.* **68,** 863–911
2. Wickner, W. (2010) Membrane fusion: five lipids, four SNAREs, three chaperones, two nucleotides, and a Rab, all dancing in a ring on yeast vacuoles. *Annu. Rev. Cell Dev. Biol.* **26,** 115–136
3. Fratti, R. A., Jun, Y., Merz, A. J., Margolis, N., and Wickner, W. (2004) Interdependent assembly of specific regulatory lipids and membrane fusion proteins into the vertex ring domain of docked vacuoles. *J. Cell Biol.* **167,** 1087–1098
4. Wang, L., Seeley, E. S., Wickner, W., and Merz, A. J. (2002) Vacuole fusion at a ring of vertex docking sites leaves membrane fragments within the organelle. *Cell* **108,** 357–369
5. Wang, L., Merz, A. J., Collins, K. M., and Wickner, W. (2003) Hierarchy of protein assembly at the vertex ring domain for yeast vacuole docking and fusion. *J. Cell Biol.* **160,** 365–374
6. Cabrera, M., Ostrowicz, C. W., Mari, M., LaGrassa, T. J., Reggiori, F., and Ungermann, C. (2009) Vps41 phosphorylation and the Rab Ypt7 control the targeting of the HOPS complex to endosome-vacuole fusion sites. *Mol. Biol. Cell* **20,** 1937–1948
7. Sasser, T., Qiu, Q. S., Karunakaran, S., Padolina, M., Reyes, A., Flood, B., Smith, S., Gonzales, C., and Fratti, R. A. (2012) Yeast lipin 1 orthologue Pah1p regulates vacuole homeostasis and membrane fusion. *J. Biol. Chem.* **287,** 2221–2236
8. Jun, Y., Fratti, R. A., and Wickner, W. (2004) Diacylglycerol and its formation by phospholipase C regulate Rab- and SNARE-dependent yeast vacuole fusion. *J. Biol. Chem.* **279,** 53186–53195
9. Schu, P. V., Takegawa, K., Fry, M. J., Stack, J. H., Waterfield, M. D., and Emr, S. D. (1993) Phosphatidylinositol 3-kinase encoded by yeast *VPS34* gene essential for protein sorting. *Science* **260,** 88–91
10. Qiu, Q. S., and Fratti, R. A. (2010) The Na^+/H^+ exchanger Nhx1p regulates the initiation of *Saccharomyces cerevisiae* vacuole fusion. *J. Cell Sci.* **123,** 3266–3275
11. Sasser, T. L., Padolina, M., and Fratti, R. A. (2012) The yeast vacuolar ABC transporter Ybt1p regulates membrane fusion through Ca^{2+} transport modulation. *Biochem. J.* **448,** 365–372
12. Gulshan, K., and Moye-Rowley, W. S. (2011) Vacuolar import of phosphatidylcholine requires the ATP-binding cassette transporter Ybt1. *Traffic* **12,** 1257–1268
13. Ortiz, D. F., St Pierre, M. V., Abdulmessih, A., and Arias, I. M. (1997) A yeast ATP-binding cassette-type protein mediating ATP-dependent bile acid transport. *J. Biol. Chem.* **272,** 15358–15365
14. Szczypka, M. S., Wemmie, J. A., Moye-Rowley, W. S., and Thiele, D. J. (1994) A yeast metal resistance protein similar to human cystic fibrosis transmembrane conductance regulator (CFTR) and multidrug resistance-associated protein. *J. Biol. Chem.* **269,** 22853–22857
15. Wemmie, J. A., and Moye-Rowley, W. S. (1997) Mutational analysis of the *Saccharomyces cerevisiae* ATP-binding cassette transporter protein Ycf1p. *Mol. Microbiol.* **25,** 683–694
16. Petrovic, S., Pascolo, L., Gallo, R., Cupelli, F., Ostrow, J. D., Goffeau, A., Tiribelli, C., and Bruschi, C. V. (2000) The products of *YCF1* and *YLL015w* (*BPT1*) cooperate for the ATP-dependent vacuolar transport of unconjugated bilirubin in *Saccharomyces cerevisiae*. *Yeast* **16,** 561–571
17. Paumi, C. M., Chuk, M., Snider, J., Stagljar, I., and Michaelis, S. (2009) ABC transporters in *Saccharomyces cerevisiae* and their interactors: new technology advances the biology of the ABCC (MRP) subfamily. *Microbiol. Mol. Biol. Rev.* **73,** 577–593
18. Paumi, C. M., Menendez, J., Arnoldo, A., Engels, K., Iyer, K. R., Thaminy, S., Georgiev, O., Barral, Y., Michaelis, S., and Stagljar, I. (2007) Mapping protein-protein interactions for the yeast ABC transporter Ycf1p by integrated split-ubiquitin membrane yeast two-hybrid analysis. *Mol. Cell* **26,** 15–25
19. Gillooly, D. J., Morrow, I. C., Lindsay, M., Gould, R., Bryant, N. J., Gaullier, J. M., Parton, R. G., and Stenmark, H. (2000) Localization of phosphatidylinositol 3-phosphate in yeast and mammalian cells. *EMBO J.* **19,** 4577–4588
20. Fratti, R. A., Collins, K. M., Hickey, C. M., and Wickner, W. (2007) Stringent 3Q.1R composition of the SNARE 0-layer can be bypassed for fusion by compensatory SNARE mutation or by lipid bilayer modification. *J. Biol. Chem.* **282,** 14861–14867
21. Fratti, R. A., and Wickner, W. (2007) Distinct targeting and fusion functions of the PX and SNARE domains of yeast vacuolar Vam7p. *J. Biol. Chem.* **282,** 13133–13138
22. Haas, A., Scheglmann, D., Lazar, T., Gallwitz, D., and Wickner, W. (1995) The GTPase Ypt7p of *Saccharomyces cerevisiae* is required on both part-

[4] T. L. Sasser and R. A. Fratti, unpublished data.

ner vacuoles for the homotypic fusion step of vacuole inheritance. *EMBO J.* **14,** 5258–5270
23. Longtine, M. S., McKenzie, A., 3rd, Demarini, D. J., Shah, N. G., Wach, A., Brachat, A., Philippsen, P., and Pringle, J. R. (1998) Additional modules for versatile and economical PCR-based gene deletion and modification in *Saccharomyces cerevisiae*. *Yeast* **14,** 953–961
24. Goldstein, A. L., Pan, X., and McCusker, J. H. (1999) Heterologous URA3MX cassettes for gene replacement in *Saccharomyces cerevisiae*. *Yeast* **15,** 507–511
25. Sokal, R. R., and Rohlf, F. J. (1994) *Biometry: The Principles and Practice of Statistics in Biological Research*, W. H. Freeman, New York
26. Collins, K. M., and Wickner, W. T. (2007) *trans*-SNARE complex assembly and yeast vacuole membrane fusion. *Proc. Natl. Acad. Sci. U.S.A.* **104,** 8755–8760
27. Jun, Y., and Wickner, W. (2007) Assays of vacuole fusion resolve the stages of docking, lipid mixing, and content mixing. *Proc. Natl. Acad. Sci. U.S.A.* **104,** 13010–13015
28. Rigaut, G., Shevchenko, A., Rutz, B., Wilm, M., Mann, M., and Séraphin, B. (1999) A generic protein purification method for protein complex characterization and proteome exploration. *Nat. Biotechnol.* **17,** 1030–1032
29. Tarassov, K., Messier, V., Landry, C. R., Radinovic, S., Serna Molina, M. M., Shames, I., Malitskaya, Y., Vogel, J., Bussey, H., and Michnick, S. W. (2008) An *in vivo* map of the yeast protein interactome. *Science* **320,** 1465–1470
30. Stroupe, C., Collins, K. M., Fratti, R. A., and Wickner, W. (2006) Purification of active HOPS complex reveals its affinities for phosphoinositides and the SNARE Vam7p. *EMBO J.* **25,** 1579–1589
31. Ungermann, C., and Wickner, W. (1998) Vam7p, a vacuolar SNAP-25 homolog, is required for SNARE complex integrity and vacuole docking and fusion. *EMBO J.* **17,** 3269–3376
32. Cheever, M. L., Sato, T. K., de Beer, T., Kutateladze, T. G., Emr, S. D., and Overduin, M. (2001) Phox domain interaction with PtdIns(3)P targets the Vam7 t-SNARE to vacuole membranes. *Nat. Cell Biol.* **3,** 613–618
33. Thorngren, N., Collins, K. M., Fratti, R. A., Wickner, W., and Merz, A. J. (2004) A soluble SNARE drives rapid docking, bypassing ATP and Sec17/18p for vacuole fusion. *EMBO J.* **23,** 2765–2776
34. Merz, A. J., and Wickner, W. (2004) *trans*-SNARE interactions elicit Ca^{2+} efflux from the yeast vacuole lumen. *J. Cell Biol.* **164,** 195–206
35. Peters, C., and Mayer, A. (1998) Ca^{2+}/calmodulin signals the completion of docking and triggers a late step of vacuole fusion. *Nature* **396,** 575–580
36. Burd, C. G., and Emr, S. D. (1998) Phosphatidylinositol (3)-phosphate signaling mediated by specific binding to RING FYVE domains. *Mol. Cell* **2,** 157–162
37. Vida, T. A., and Emr, S. D. (1995) A new vital stain for visualizing vacuolar membrane dynamics and endocytosis in yeast. *J. Cell Biol.* **128,** 779–792
38. Li, Z. S., Szczypka, M., Lu, Y. P., Thiele, D. J., and Rea, P. A. (1996) The yeast cadmium factor protein (YCF1) is a vacuolar glutathione *S*-conjugate pump. *J. Biol. Chem.* **271,** 6509–6517
39. Gueldry, O., Lazard, M., Delort, F., Dauplais, M., Grigoras, I., Blanquet, S., and Plateau, P. (2003) Ycf1p-dependent Hg(II) detoxification in *Saccharomyces cerevisiae*. *Eur. J. Biochem.* **270,** 2486–2496
40. Lee, M. E., Singh, K., Snider, J., Shenoy, A., Paumi, C. M., Stagljar, I., and Park, H. O. (2011) The Rho1 GTPase acts together with a vacuolar glutathione *S*-conjugate transporter to protect yeast cells from oxidative stress. *Genetics* **188,** 859–870
41. Eitzen, G., Thorngren, N., and Wickner, W. (2001) Rho1p and Cdc42p act after Ypt7p to regulate vacuole docking. *EMBO J.* **20,** 5650–5666
42. Eitzen, G., Wang, L., Thorngren, N., and Wickner, W. (2002) Remodeling of organelle-bound actin is required for yeast vacuole fusion. *J. Cell Biol.* **158,** 669–679
43. Karunakaran, S., Sasser, T., Rajalekshmi, S., and Fratti, R. A. (2012) SNAREs, HOPS and regulatory lipids control the dynamics of vacuolar actin during homotypic fusion in *S. cerevisiae*. *J. Cell Sci.* **125,** 1683–1692
44. Boeddinghaus, C., Merz, A. J., Laage, R., and Ungermann, C. (2002) A cycle of Vam7p release from and PtdIns 3-P-dependent rebinding to the yeast vacuole is required for homotypic vacuole fusion. *J. Cell Biol.* **157,** 79–89
45. Karunakaran, S., and Fratti, R. (2013) The lipid composition and physical properties of the yeast vacuole affect the hemifusion-fusion transition. *Traffic* **14,** 650–662
46. Parrish, W. R., Stefan, C. J., and Emr, S. D. (2004) Essential role for the myotubularin-related phosphatase Ymr1p and the synaptojanin-like phosphatases Sjl2p and Sjl3p in regulation of phosphatidylinositol 3-phosphate in yeast. *Mol. Biol. Cell* **15,** 3567–3579
47. Yamamoto, A., DeWald, D. B., Boronenkov, I. V., Anderson, R. A., Emr, S. D., and Koshland, D. (1995) Novel PI(4)P 5-kinase homologue, Fab1p, essential for normal vacuole function and morphology in yeast. *Mol. Biol. Cell* **6,** 525–539
48. Bonangelino, C. J., Nau, J. J., Duex, J. E., Brinkman, M., Wurmser, A. E., Gary, J. D., Emr, S. D., and Weisman, L. S. (2002) Osmotic stress-induced increase of phosphatidylinositol 3,5-bisphosphate requires Vac14p, an activator of the lipid kinase Fab1p. *J. Cell Biol.* **156,** 1015–1028
49. Efe, J. A., Botelho, R. J., and Emr, S. D. (2005) The Fab1 phosphatidylinositol kinase pathway in the regulation of vacuole morphology. *Curr. Opin. Cell Biol.* **17,** 402–408
50. Michell, R. H., Heath, V. L., Lemmon, M. A., and Dove, S. K. (2006) Phosphatidylinositol 3,5-bisphosphate: metabolism and cellular functions. *Trends Biochem. Sci.* **31,** 52–63
51. Mayer, A., Scheglmann, D., Dove, S., Glatz, A., Wickner, W., and Haas, A. (2000) Phosphatidylinositol 4,5-bisphosphate regulates two steps of homotypic vacuole fusion. *Mol. Biol. Cell* **11,** 807–817
52. Hall, A. (1998) Rho GTPases and the actin cytoskeleton. *Science* **279,** 509–514
53. Ganeshan, R., Di, A., Nelson, D. J., Quick, M. W., and Kirk, K. L. (2003) The interaction between syntaxin 1A and cystic fibrosis transmembrane conductance regulator Cl^- channels is mechanistically distinct from syntaxin 1A-SNARE interactions. *J. Biol. Chem.* **278,** 2876–2885
54. Short, D. B., Trotter, K. W., Reczek, D., Kreda, S. M., Bretscher, A., Boucher, R. C., Stutts, M. J., and Milgram, S. L. (1998) An apical PDZ protein anchors the cystic fibrosis transmembrane conductance regulator to the cytoskeleton. *J. Biol. Chem.* **273,** 19797–19801
55. Bared, S. M., Buechler, C., Boettcher, A., Dayoub, R., Sigruener, A., Grandl, M., Rudolph, C., Dada, A., and Schmitz, G. (2004) Association of ABCA1 with syntaxin 13 and flotillin-1 and enhanced phagocytosis in tangier cells. *Mol. Biol. Cell* **15,** 5399–5407
56. Jones, E. W., Zubenko, G. S., and Parker, R. R. (1982) *PEP4* gene function is required for expression of several vacuolar hydrolases in *Saccharomyces cerevisiae*. *Genetics* **102,** 665–677
57. Haas, A., Conradt, B., and Wickner, W. (1994) G-protein ligands inhibit *in vitro* reactions of vacuole inheritance. *J. Cell Biol.* **126,** 87–97